

# Characteristic of a Broadband Ti:LiNbO<sub>3</sub> Optical Modulator with Buried Electrodes and Etched Grooves in the Buffer Layer

JINYANG HU  
BOYU WU  
XIAOMIN JIN

Electronic Engineering Department  
Tsinghua University  
Beijing, China

*Traveling wave Ti:LiNbO<sub>3</sub> Mach-Zehnder optical modulators with buried electrodes and etched grooves in the SiO<sub>2</sub> buffer layer are analyzed by the finite element method. The tradeoff between the bandwidth  $BW$  and the half-wave voltage  $V_{\pi}$  is discussed. The value of  $BW/V_{\pi}$  is used to weight the total performance of the modulator. Taking a thick buffer layer and etching deep grooves in the buffer layer are demonstrated as two effective methods to improve the performance of the modulator. A 3-dB optical bandwidth of 18 GHz with half-wave voltage 5V at a wavelength of 1.55  $\mu\text{m}$  could be obtained even though the electrode is not very thick. When the requirement of half-wave voltage is not very critical, a bandwidth of more than 100 GHz can be obtained.*

**Keywords** FEM analysis, integrated optics, modulator, optical waveguide, Ti:LiNbO<sub>3</sub>

The important parameters of an electro-optical modulator are the modulation bandwidth  $BW$  and the half-wave voltage  $V_{\pi}$ . Broadband operation is necessary for high-speed optical fiber communication. High half-wave voltage will prevent its practical application. A larger value of  $BW/V_{\pi}$  indicates better total performance of the modulator.

The modulation bandwidth can be expanded by taking some velocity-matched structures. Using thick electrodes in conjunction with a thick buffer layer is the most simple and effective way [1]. The half-wave voltage can be reduced by decreasing the distance between the electrodes and the waveguides because it increases the interaction between the microwave and the optical wave. Adapting the structure of buried electrodes is very efficient [2]. To obtain a low half-wave voltage, the bottom of the buried electrodes must be near the optical waveguides. In this condition, the modulator works under the velocity-mismatched state and results in a narrower bandwidth. Therefore, there is a tradeoff between the modulation bandwidth and the half-wave voltage. To compensate for the decrease of bandwidth, etching grooves in the buffer layer is recommended.

The *finite element method* (FEM) is used to design the Ti:LiNbO<sub>3</sub> optical modulator with buried electrodes and etched grooves in the buffer layer in this paper. The configuration parameters with comparatively good  $BW/V_\pi$  performance are obtained in the end.

## Design and Calculation

The cross-section view of the Mach–Zehnder optical-intensive modulator is shown in Figure 1. Titanium indiffused waveguides are formed in a Z-cut LiNbO<sub>3</sub> substrate. The substrate is coated with a buffer layer of silicon oxide. A *coplanar waveguide* (CPW) electrode is formed on the buffer layer by gold-electroplating. Some parts of the CPW electrode are buried in the buffer layer to increase the electro-optic interaction. Etching grooves in the buffer layer expand the bandwidth when the modulator works under the velocity-mismatched state.

In order to make the characteristic impedance near 50  $\Omega$ , hot electrode width  $W$ , gap  $G$ , and the width of the buried electrodes  $W_b$  are 10  $\mu\text{m}$ , 23  $\mu\text{m}$ , and 4  $\mu\text{m}$ , respectively. The interaction length is 25 mm. The electrode thickness  $T$  is 15  $\mu\text{m}$ . The SiO<sub>2</sub> buffer layer thickness  $H$  is 3  $\mu\text{m}$ . The optical mode size is 8  $\mu\text{m}$  in the FEM calculations because this value is well fit to the  $V_\pi$ 's measurement in our laboratory. The modulator is designed at 1.55  $\mu\text{m}$  optical wavelength.

The width of the buried part of the electrode is narrower than that of the upper part. It results in a more concentrated microwave electric field around the optical waveguide and a stronger effective interaction between the microwave and the optical wave. So the depth of the buried electrodes is a key parameter in our design.

There are a lot of mathematical methods in the analyses of the conventional modulators. As to the complex configuration of the modulator discussed in this letter, the FEM is the best [3].

We employ the FEM calculation software in our work that was made in our laboratory previously. Both velocity mismatching and conductor loss are considered in the bandwidth calculations in this software. The treatment of conductor loss  $\alpha_0$  in this paper is based on the “incremental inductance rule” of Wheeler [4]. The formula is

$$\alpha_0 = \frac{1}{2Z_{0m}} \sqrt{\frac{\epsilon_0}{\mu_0}} \sum_m \sqrt{\pi\mu_m \rho} \frac{\partial Z_{0m}^a}{\partial n_m} \quad (\text{nepers/unit length}) \quad (1)$$

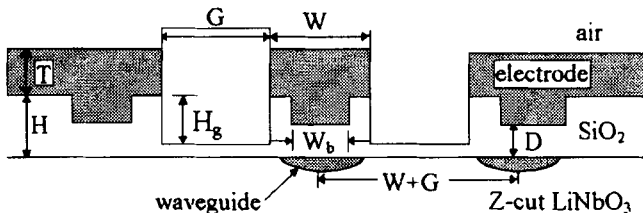


**Figure 1.** Cross section of the modulator with buried electrodes and etched grooves in buffer layer.

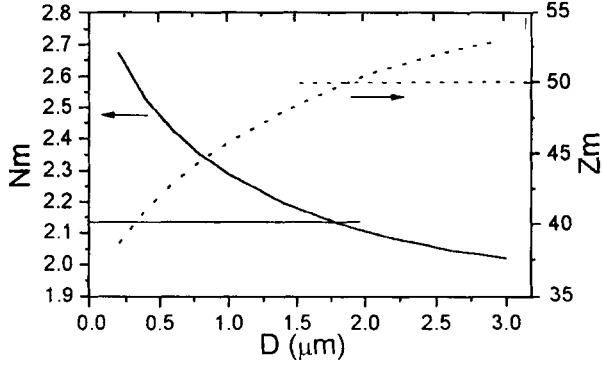


**Figure 2.** Relationship of  $N_m$  and  $Z_m$  with parameter of  $D$  when  $H = 3 \mu\text{m}$  and  $T = 15 \mu\text{m}$ .

where  $Z_{0m}^a$  is the free-space characteristic impedance of electrodes.  $\partial Z_{0m}^a / \partial n_m$  denotes the derivative of  $Z_{0m}^a$  with respect to incremental recession of electrode surfaces wall  $m$ .  $\rho$  is the metal resistivity.  $Z_{0m}$  is the characteristic impedance of electrodes. For Au electrodes, the formula is

$$\alpha_0 = 1.1314 \frac{1}{Z_{0m}} \sum_m \frac{\partial Z_{0m}^a}{\partial n_m} \quad (\text{dB}/\text{GHz}^{1/2} \text{ cm}) \quad (2)$$

FEM calculations shown in Figure 2 indicate the changes of the microwave effective index  $N_m$  and the characteristic impedance  $Z_m$  against  $D$  (the distance between the bottom of the buried electrodes and the surface of the substrate). When  $D$  decreases, which means the buried electrodes become closer to the optical waveguides,  $N_m$  increases and  $Z_m$  decreases. When  $D$  is around  $1.7 \mu\text{m}$ , both  $N_m$  and  $Z_m$  reach optimum values: the velocity of the microwave matches that of the optical wave and the characteristic impedance of the traveling wave electrodes equals  $50 \Omega$ .

Figure 3 is the graph of conductor loss  $\alpha_0$  versus  $D$ . When the buried electrodes become closer to the substrate, the conductor loss increases.

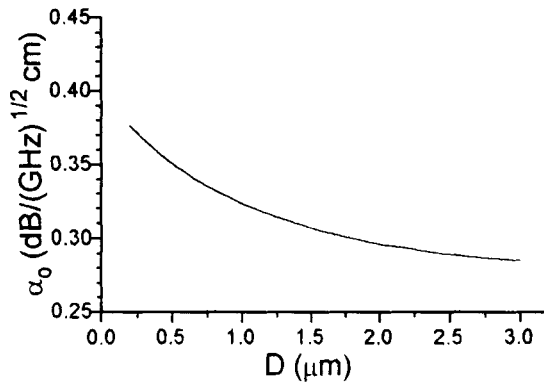


**Figure 3.** Relationship of  $\alpha_0$  with parameter of  $D$  when  $H = 3 \mu\text{m}$  and  $T = 15 \mu\text{m}$ .

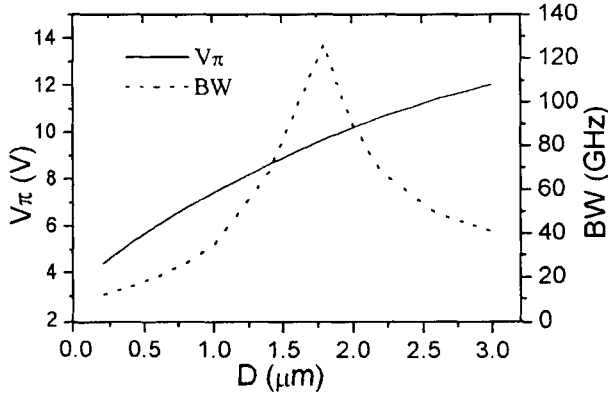


**Figure 4.** Relationship of  $V_{\pi}$  and  $BW$  with parameter of  $D$  when  $H = 3 \mu\text{m}$  and  $T = 15 \mu\text{m}$ .

Figure 4 shows the curves of the 3-dB optical modulation bandwidth  $BW$  and the half-wave voltage  $V_{\pi}$  with the parameter of  $D$ . In the velocity-matched region ( $1.6 \mu\text{m} < D < 1.9 \mu\text{m}$ ),  $BW$  exceeds 100 GHz while  $V_{\pi}$  is about 10V. Figure 5 shows the curve of  $BW/V_{\pi}$  against  $D$ . It demonstrates that  $BW/V_{\pi}$  reaches its maximum value at the velocity-matched point ( $D \approx 1.7 \mu\text{m}$ ) and that in the velocity-matched region ( $1.6 \mu\text{m} < D < 1.9 \mu\text{m}$ )  $BW/V_{\pi}$  is over 10 GHz/V.

But a  $V_{\pi}$  of about 10V is still high for a practical application. A driving source that can supply such a high voltage is too expensive. A convenient value of  $V_{\pi}$  is about 5V. Referring to Figure 4, the corresponding  $D$  is around  $0.4 \mu\text{m}$ . For this design, the conductor loss is  $0.357 \text{ dB/GHz}^{0.5} \text{ cm}$  and the bandwidth is about 15 GHz.

Figure 4 also shows that  $V_{\pi}$  falls approximately linear as  $D$  decreases.  $V_{\pi}$  is mainly decided by  $D$ . When  $D$  is fixed,  $V_{\pi}$  does not change much even when the thickness of the buffer layer  $H$  changes as shown in the left part of Figure 6. It also shows that  $BW$  increases almost linearly with  $H$ . From this, we know that increasing the buffer layer thickness is an effective way to improve the  $BW/V_{\pi}$  performance of the modulator (referring to the left side of Figure 7).

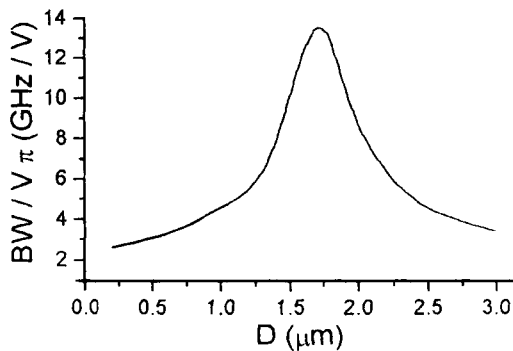


**Figure 5.** Relationship of  $BW/V_{\pi}$  with parameter of  $D$  when  $H = 3 \mu\text{m}$  and  $T = 15 \mu\text{m}$ .

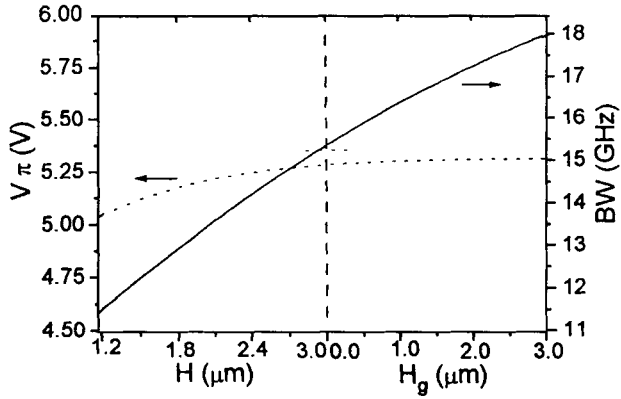


**Figure 6.** Relationship of  $V_\pi$  and  $BW$  with parameter of  $H$  (in the left part) and  $H_g$  (in the right part) when  $D = 0.4 \mu\text{m}$  and  $T = 15 \mu\text{m}$ .

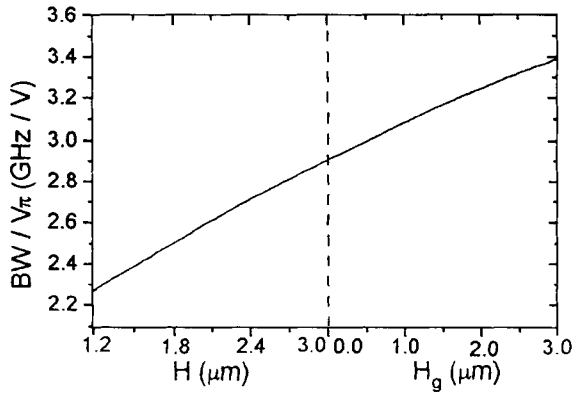


**Figure 7.** Relationship of  $BW/V_\pi$  with parameter of  $H$  (in the left part) and  $H_g$  (in the right part) when  $D = 0.4 \mu\text{m}$  and  $T = 15 \mu\text{m}$ .

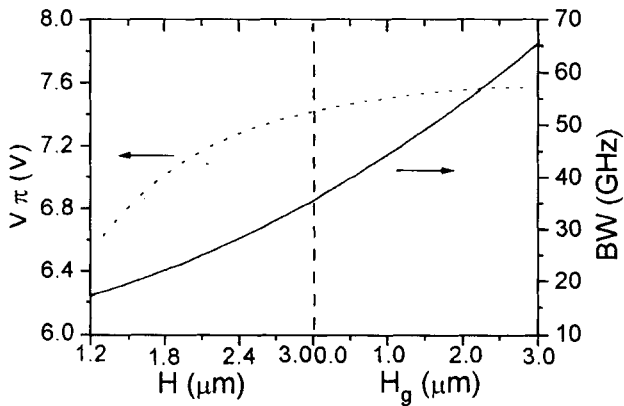


**Figure 8.** Relationship of  $V_\pi$  and  $BW$  with parameter of  $H$  (in the left part) and  $H_g$  (in the right part) when  $D = 1.0 \mu\text{m}$  and  $T = 15 \mu\text{m}$ .

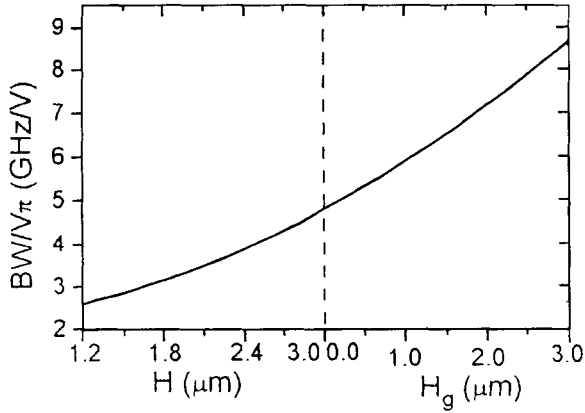


**Figure 9.** Relationship of  $BW/V_\pi$  with parameter of  $H$  (in the left part) and  $H_g$  (in the right part) when  $D = 1.0 \mu\text{m}$  and  $T = 15 \mu\text{m}$ .

Etching grooves in the  $\text{SiO}_2$  buffer layer at the gap will increase the modulation bandwidth, meanwhile the half-wave voltage even does not change. The calculation results are shown in the right side of Figure 6, where  $H_g$  is the depth of the grooves. Referring to the right part of Figure 7, etching grooves is another effective method to improve the  $BW/V_\pi$  performance.

Referring to Figure 6, we also find the increase in the modulation bandwidth is small. The reason is that this design is seriously velocity mismatched ( $D = 0.4 \mu\text{m}$  and  $N_m = 2.53$  in Figure 2). Increasing  $D$  to  $1.0 \mu\text{m}$  will make a distinctive improvement ( $N_m = 2.29$ ). The conductor loss is  $0.324 \text{ dB/GHz}^{0.5} \text{ cm}$  for this design. The calculation results are shown in Figures 8 and 9 when all parameters are kept the same as those in Figure 6 except  $D$  is increased to  $1.0 \mu\text{m}$ .  $V_\pi$  is about  $7\text{V}$  as  $BW$  changes from  $18 \text{ GHz}$  to  $65 \text{ GHz}$ . An increase in the modulation bandwidth is much larger than the upper design ( $D = 0.4 \mu\text{m}$ ). Of course, it is the consequence of the tradeoff done to improve  $V_\pi$ .

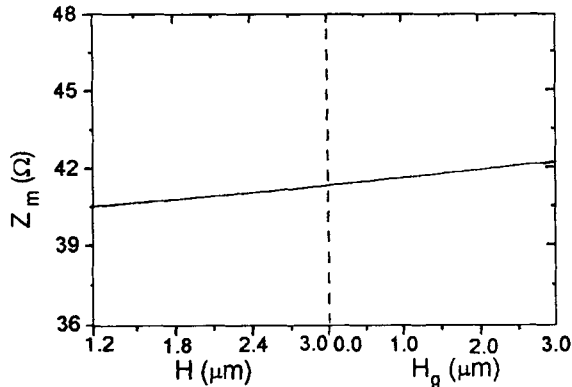


**Figure 10.** Relationship of  $Z_m$  with parameter of  $H$  (in the left part) and  $H_g$  (in the right part) when  $D = 0.4 \mu\text{m}$  and  $T = 15 \mu\text{m}$ .

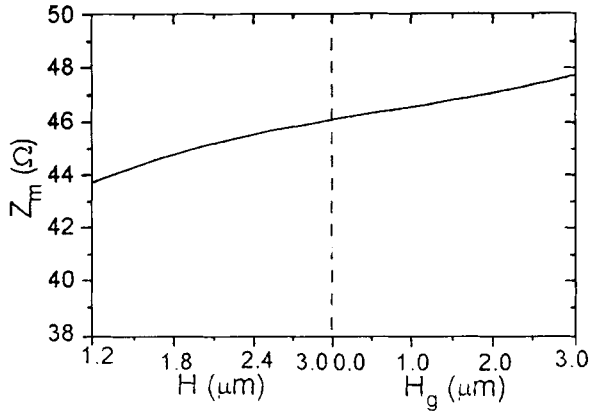


**Figure 11.** Relationship of  $Z_m$  with parameter of  $H$  (in the left part) and  $H_g$  (in the right part) when  $D = 1.0 \mu\text{m}$  and  $T = 15 \mu\text{m}$ .

In addition, the characteristic impedances in the calculations mentioned are more than  $40 \Omega$ , as shown in Figure 10 ( $D = 0.4 \mu\text{m}$ ) and Figure 11 ( $D = 1.0 \mu\text{m}$ ), so it is easy to achieve the impedance match in the modulator design.

## Conclusion

In conclusion, we obtain a model of an optical modulator using buried electrodes and etched grooves in the buffer layer. The tradeoff between the bandwidth and the half-wave voltage is taken into account and is judged by the value of  $BW/V_\pi$ . A modulator with a bandwidth of more than 100 GHz and a  $V_\pi$  of 10V can be obtained when  $D$  is  $1.7 \mu\text{m}$ ,  $H$  is  $3 \mu\text{m}$ , and  $T$  is  $15 \mu\text{m}$ . For practical application,  $D$  is designed as  $0.4 \mu\text{m}$  to achieve a low enough half-wave voltage. In this condition, the modulator works under the velocity-mismatched state and results in a bandwidth decrease. Etching grooves in the buffer layer is taken as compensation. The following dimensions can lead to a bandwidth of 18 GHz with a half-wave voltage of 5V:  $T = 15 \mu\text{m}$ ,  $H = 3 \mu\text{m}$ ,  $H_g = 3 \mu\text{m}$ ,  $D = 0.4 \mu\text{m}$ .

## References

1. Gopalakrishnan, G. K., C. H. Bulmer, W. K. Burns, R. W. Mcelhanon, and A. S. Greenblatt. 1992. 40 GHz, low half-wave voltage Ti:LiNbO<sub>3</sub> intensity modulator. *Electron. Lett.*, 28:826–827.
2. Miyamoto, H., H. Ohta, K. Tabuse, and Y. Miyagawa. 1992. Design of high efficiency LiNbO<sub>3</sub> broadband phase modulator using an electrode buried in buffer layer. *Electron. Lett.* 28:322–324.
3. Yi, J. C. 1990. Finite element method for the impedance analysis of traveling-wave modulators. *J. Lightwave Tech.* 8.
4. Wheeler, H. A. 1942. Formulas for the skin effect. *Proc. IRE* 30:412–424.

## Biographies

**Jinyang Hu** was born in August, 1973. He received the B.Sc. degree in Electronics Engineering from the University of Tsinghua, Beijing, China in 1995. Now he is a graduated student in the Electronic Engineering Department of Tsinghua University. He has been engaged in research on integrated optical components and fiber communication systems.

**Boyu Wu** was born in February, 1939. He graduated from the Department of Radio-Electronic, Tsinghua University, Beijing, China in 1962. From 1962 to 1983 he was engaged in research of microwave electronics. Since 1983 he has been engaged in the research of integrated optics and optical components and systems. His current technical interests include high-speed optical modulator/switches, broadband optical fiber communications. Professor Wu is a member of Electronic Society of China and the Optical Society of America.

**Xiaomin Jin** received the B.Sc. and M.Sc. degrees in Electronics Engineering from the University of Tsinghua, Beijing, China, in 1992 and 1996, respectively. Since 1991 she was engaged in research on optical components, such as external optical modulators and tunable acousto-optic filters. She is a student member of IEEE.